The Dissolution Kinetics of Fe_3C in Ferrite – A Theory of Interface Migration

FRANK V. NOLFI, Jr., PAUL G. SHEWMON, and JAMES S. FOSTER

The dissolution of Fe_3C in ferrite has been shown to be controlled by a slow first order interfacial reaction. The rate constant, K, is Arrhenius in behavior and involves two activation enthalpies; one applies to a jump process with a short relaxation time, another to a long relaxation time process which is tentatively identified as a change in kink density on ledges in the interface. The heat of solution of Fe_3C in ferrite also appears in the exponential. A single process, activated jump theory is not adequate to explain the behavior of K with temperature; a dissolution model based on a ledge-double kink mechanism appears to be in agreement with experiment. These features point to significant differences between the mechanism of interphase boundary migration and grain boundary migration. In addition, the Fe_3C-ferrite interface is felt to be at equilibrium with respect to carbon but not iron, leading to small departures from stoichiometry in the Fe_3C at the interface.

In a previous paper, Nolfi *et al.*[1] have derived equations applicable to the dissolution of spheroidized cementite in ferrite when a) local equilibrium does or does not exist at the Fe_3C-ferrite interface and b) the nonequilibrium condition is characterized by a carbon flux across the interface which is proportional to the deviation from equilibrium. Specifically

$$J_{R=R_0} = -K(C_S - C_{eq}) \qquad [1]$$

where $J_{R=R_0}$ is the carbon flux at the particle-matrix interface, R_0 is the mean radius of the precipitate particles, K is the reaction rate constant, and C_S and C_{eq} are, respectively, the actual and equilibrium concentrations of carbon in the ferrite at the interface. Fig. 1 depicts the two possible conditions at the interface corresponding to local equilibrium and nonequilibrium (C_{CPD} is the carbon concentration of Fe_3C). The value of $(C_S - C_{eq})$ is reflected in the parameter $0 \leq \sigma \leq 1$ where $\sigma = 0$ corresponds to interfacial equilibrium ($C_S = C_{eq} : K = \infty$) and $\sigma = 1$ corresponds to a zero reaction rate ($K = 0$). In the latter case C_S equals the initial carbon concentration C_∞ and remains there so that $C_S - C_{eq} = C_\infty - C_{eq} = -\Delta C_0$. On the basis of this model the rate of change of the average carbon concentration in ferrite is

$$\dot{\bar{C}}(t) = \Delta C_0 \sum_{n=0}^{\infty} G_n \exp(-t/\tau_n) \qquad [2]$$

where the G_n's are constants for isothermal dissolution and the τ_n's are a sequence of decreasing relaxation times given by

$$1/\tau_n = \left(\frac{\alpha_n \beta}{R_0}\right)^2 D \qquad [3]$$

where D is the solute diffusivity in the matrix, $\beta \equiv (f_p)^{1/3}$ (f_p is the volume fraction of precipitate) and the α_n's are defined by

$$\alpha_n(1-\beta) = \tan^{-1}\left|\frac{\alpha_n(1-\sigma\beta)}{1+\sigma\beta\alpha_n^2}\right| + n\pi, \quad n = 0, 1, 2, \ldots \qquad [4]$$

After sufficient time, t is very much greater than τ_n for all τ_n except τ_0 and Eq. [2] becomes

$$\dot{\bar{C}}(t) = \Delta C_0 G_0 \exp(-t/\tau_0) \qquad [5]$$

From Eqs. [3] and [4], it is clear that $1/\tau_0$ defines σ (R_0, β, and D are independently measurable) and hence the rate controlling process for dissolution. In addition, σ is defined by

$$\sigma = \left(\frac{KR_0}{D} + 1\right)^{-1} \qquad [6]$$

and its determination also determines K.

In another paper, Nolfi *et al.*[2] have presented experimental measurements of τ_0 and σ which show that the isothermal dissolution kinetics of Fe_3C in ferrite are strongly controlled by a slow first order interfacial

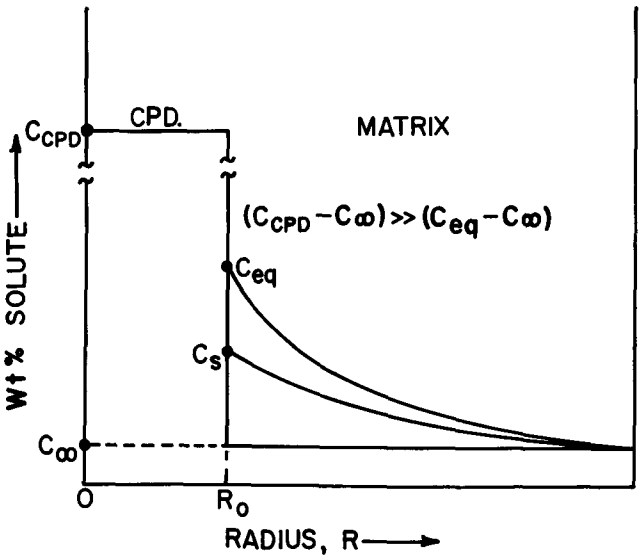

Fig. 1—Schematic diagram of possible solute concentration profiles in the matrix near the particle-matrix interface during dissolution.

FRANK V. NOLFI, JR., formerly Graduate Student, Department of Metallurgy and Materials Science, Carnegie-Mellon University, Pittsburgh, Pa., is Assistant Metallurgist, Argonne National Laboratory, Argonne, Ill. PAUL G. SHEWMON is Division Director, Materials Science Division, Argonne National Laboratory. JAMES S. FOSTER is Assistant Professor, Department of Metallurgy and Materials Science, Carnegie-Mellon University. This paper is based on a thesis submitted by FRANK V. NOLFI, JR. in partial fulfillment of the requirements of the degree of Doctor of Philosophy at Carnegie-Mellon University.

Manuscript submitted October 13, 1969.

reaction rather than by long range diffusion of carbon or iron, as evidenced by measured values of σ in the range of 0.932 to 0.997. From these data, calculations of K were made and found to be in the range of 0.84 to 2.17×10^{-4} cm per sec. The experiments consisted of equilibrating wire specimens of spheroidized eutectoid steels at 650° or 700°C and then jumping the temperature (in 2 to 7 msec) 4 to 32 C° above the equilibration temperature. After heating, the specimens were maintained constant at the new temperature, and the dissolution of Fe_3C was followed by observing the changes in electrical resistivity. On an average the Fe_3C ferrite boundaries moved 30Å or less while carbon diffused over distances in the order of 10 μ in about 1 sec. The materials studied were high-purity (HP) and commercial purity (C)* eutectoid steels which had

*The composition by wt pct was 0.88C, 0.48 Mn, 0.21 Si, 0.019 S, 0.009 P.

either been recrystallized and spheroidized (RS) or quenched and spheroidized (QS).

If all of the precipitate particles present in a given specimen actually had not dissolved during an experiment, then the metallographically measured volume fraction of precipitate[2] or equivalently β[3] would be too large. Therefore, the α_0's calculated through Eq. [3] from experimentally determined τ_0's would be too small, thus causing an error in the calculation of σ through Eq. [4]. Nolfi *et al*[1] have given data based on Eq. [4] which show that for a given value of $(\alpha_0\beta)^2$ a decrease in β and corresponding increase in α_0 produces a decrease in the computed value of σ.

For example, if the actual volume fraction of precipitate undergoing dissolution in specimen HP-QS had been $(\beta^3) = 10^{-3}$ instead of the metallographically determined 0.157,[2] the calculated value of the σ's would have been close to zero, *i.e.* the kinetics would have been determined by the diffusion controlled dissolution of ~1 pct of the available precipitate. However, had this been the case Eqs. [3], [4], and [6] indicate that the determined α_0's would be independent of temperature and the $(1/\tau_0)$'s would show the temperature dependence of D. This was not observed to be the case,[2] and the conclusion of interfacial reaction controlled dissolution is maintained.

Fig. 2 shows plots of $(-\ln K)$ vs $(1/T)$, where it is seen that the data can be represented by straight lines of positive slope. In constructing this figure, the points corresponding to the lowest ΔT (indicated by circles) were not included in the least squares analyses for the slopes and intercepts because of the uncertainty in determining K for very small ΔT's. In addition, the Q values listed on the figure were obtained by multiplying the slopes by the gas constant. Table I summarizes the data shown in Fig. 2 and also gives the intercepts of each graph as determined by the least squares analyses. Further, error estimates for the Q's and intercepts are defined and given.

In the cases of specimens HP-QS and C-RS, Fig. 2 shows that there are two groups of data for each specimen. Each group corresponds to data collected by initiating the temperature jumps from a different equilibration temperature, T_0. Note that for each specimen, the data collected at $T_0 \cong 650$°C yield an essentially parallel slope to that of the data collected at $T_0 \cong 700$°C, but displaced below the higher temperature data by a constant difference (a constant factor for K). The data

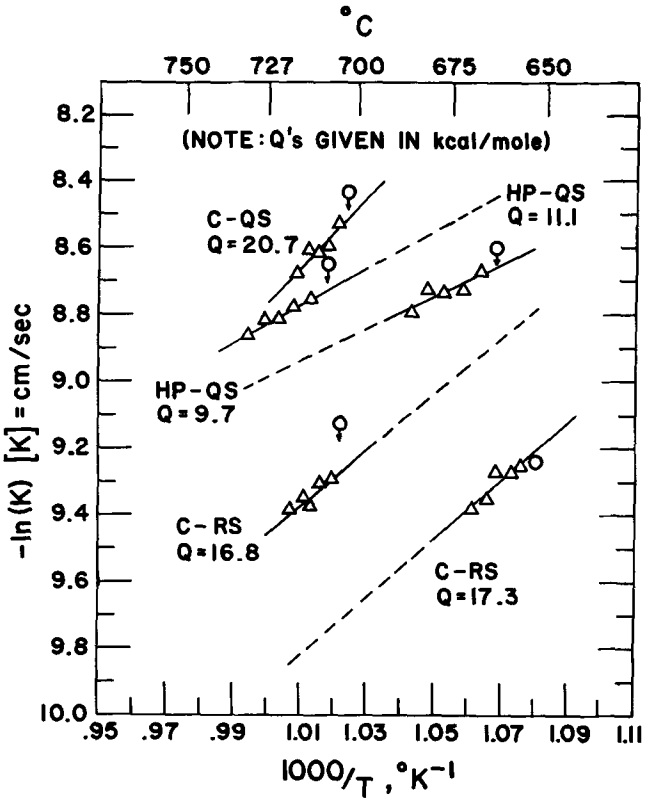

Fig. 2—Plot of $[-\ln (K)]$ vs $[1/T]$.

Table I. Summary of Data in Fig. 2 Including Values of the Intercepts and Estimated Error Limits for the Q's and the Intercepts

Sample	T_0, °C	Q, kcal/mole*	(I) Intercept, cm/sec	Intercept Error† E_1	Intercept Error† E_2
HP-QS	701	11.1 ±0.7, 3.4	5.69×10^{-7}	1.43	5.42
HP-QS	656	9.7 ±1.9, 8.9	9.89×10^{-7}	2.70	1.08×10^{2}
C-RS	701	16.8 ±2.9, 13.6	1.72×10^{-8}	4.33	1.01×10^{3}
C-RS	647	17.3 ±2 7, 12.5	8.89×10^{-9}	4.14	8.11×10^{2}
C-QS	698	20.7 ±3.2, 15.1	5.01×10^{-9}	5.08	2.12×10^{3}

*The two errors listed are, respectively, the probable error limits[3] and the 95 pct confidence limits. The probable error limits are the 50 pct confidence limits had the data set been infinite, and are slightly less than this for the actual finite set.

†E_1 and E_2 correspond, respectively, to the probable error and 95 pct confidence limits. The upper and lower limits of (I) are given by $I_i \uparrow = E_i I$ and $I_i \downarrow = I/E_i$.

in Fig. 2 and Table I also show that for a (QS) treatment, the (HP) and the (C) material have essentially the same K but the (HP) material has a lower Q than the (C) material. Also note that for the (C) material the (RS) treated specimen has a lower K than the (QS) specimen, and probably a lower value of Q.*

*The 95 pct confidence limits given in Table I show that it is possible that there are no statistical differences among any of the Q's and I's. However, Fig. 2 shows trends which indicate that the probable errors (~50 pct confidence limits) are more appropriate Therefore, all past and future discussion of the significance of various features of the data is made on the basis of the probable error limits.

THEORY

I) The Thermodynamic Driving Force

Initially, the system under discussion is in two-phase equilibrium at temperature, T_0, and the dissolu-

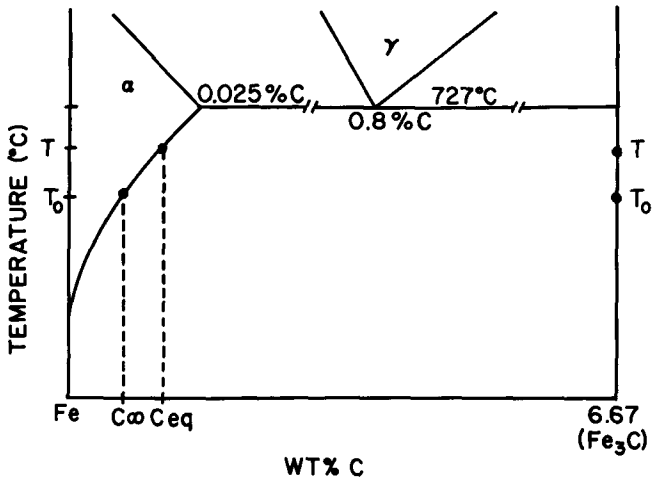

Fig. 3—Schematic diagram of pertinent portion of Fe-C phase diagram.

tion is effected by quickly changing the temperature to T and then allowing the system to relax to a new equilibrium state.[2] It is apparent that the thermodynamic driving force for the reaction is brought about by the temperature jump (herein T-jump). This driving force will be, in the main, due to chemical changes.

At equilibrium, the chemical potentials, μ, of iron and carbon in each phase are equal. Thus,

$$\mu_C^{\alpha} = \mu_C^{Fe_3C} \quad [7a]$$

$$\mu_{Fe}^{\alpha} = \mu_{Fe}^{Fe_3C} \quad [7b]$$

where the subscript refers to the atomic species, and the superscript to the phase. The precipitate particles are assumed large enough so that capillarity effects are absent and so the phase diagram may be used to determine equilibrium compositions. Fig. 3 is a schematic drawing of the pertinent portion of the Fe-C phase diagram.

For the present it will be assumed that the Fe_3C is a stoichiometric compound of invariant carbon concentration, C_{CPD} = 6.67 wt pct. Given this, the only changes in $\mu_{Fe}^{Fe_3C}$ and $\mu_C^{Fe_3C}$ that occur are those during the T-jump since no composition relaxations occur in Fe_3C. On the other hand μ_{Fe}^{α} and μ_C^{α}, not only change during the T-jump, but also change isothermally at T when dissolution of Fe_3C causes the ferrite carbon concentration to change from C_∞ to C_{eq}.

Since ferrite of composition C_{eq} is in equilibrium with Fe_3C of composition C_{CPD}, local nonequilibrium at the interface, i.e. $\mu_C^{\alpha}(C_s) < \mu_C^{\alpha}(C_{eq})$ (Fig. 1), causes the chemical potentials of iron and carbon to be discontinuous at the interface. Since the carbon concentrations are very low, it is safe to assume that Henry's law applies for carbon and thus Raoult's law for iron.[4] Thus, the magnitude of the discontinuities can be approximated by

$$\Delta\mu_C = RT \ln C_s/C_{eq} \quad [8a]$$

$$\Delta\mu_{Fe} = RT \ln X_s/X_{eq} \quad [8b]^*$$

*In determining the signs of the discontinuities, the convention used is to consider the atoms to be going *from* the Fe_3C *to* the ferrite.

where X_s and X_{Fe} are, respectively, the mole fractions of iron in ferrite of carbon concentrations, C_s and C_{eq}; the concentrations, "C," are expressed as weight fractions or percentages.*

*Eq. [8b] has been written in terms of mole fractions because at high concentrations of iron, such as encountered in ferrite, the mole fraction is *not* related to weight fraction by a simple multiplicative constant as in Eq. [8a].

Since the changes in both carbon and iron concentrations are very small, Eqs. [8a] and [8b] may be approximated by

$$\Delta\mu_C \cong RT\left(\frac{C_s - C_{eq}}{C_{eq}}\right) \quad [9a]$$

$$\Delta\mu_{Fe} \cong -RT\left(\frac{C_s - C_{eq}}{21.4}\right) \quad [9b]$$

where the use of Eq. [9b] requires that the concentrations, C_s and C_{eq}, be expressed as weight percentages. Further, in deriving Eq. [9b] it is recognized that $C_s \ll 21.4$, since $C_s(\max) = 0.025$ wt pct.

Swartz[5] has measured the solubility of graphite in ferrite as a function of temperature and found that it obeys the relation

$$\text{wt pct } C(\alpha\text{-Gr}) = 3.35 \times 10^3 \exp(-24{,}000/RT) \quad [10]$$

this expression being valid from the eutectoid temperature to ~450°C. Swartz also finds that the ratios of cementite solubility to graphite solubility given by Darken and Gurry[4] when used in conjunction with Eq. [10] gives the correct cementite solubility over the range 600°C $\leq T \leq$ 727°C. These ratios are found from a least squares analysis to follow the expression

$$\frac{\text{wt pct C}(\alpha\text{-Gr.})}{\text{wt pct C}(\alpha\text{-}Fe_3C)} = 26.0 \exp(-6.69 \times 10^3/RT) \quad [11]$$

over the temperature range 700°K $\leq T \leq$ 1000°K. The cementite solubility is, therefore, from Eqs. [10] and [11]

$$\text{wt pct C}(\alpha\text{-}Fe_3C) = 1.29 \times 10^2 \exp(-17.3 \times 10^3/RT) \quad [12]$$

Fig. 4 shows a schematic representation of the chemical potentials of iron and carbon at the interface assuming a situation where $C_s = C_\infty$. This would correspond to a value of $K = 0$. The arrows indicate the direction μ_C^{α} and μ_{Fe}^{α} will move during the dissolution. Particularly noteworthy is that iron experiences a small but finite increase in its chemical potential in moving across the interface from Fe_3C to ferrite. As an example, if it is assumed that $K = 0$ and a T-jump of 30C° has occurred from T_0 = 700°C, then $\Delta\mu_C$ = −534 cal per mole and $\Delta\mu_{Fe}$ = +0.47 cal per mole.

Cementite has a volume per iron atom which is 9 pct higher than that of iron in ferrite.[6] Thus, during precipitation or dissolution internal stresses are developed which could, if of sufficient magnitude, alter significantly the driving force for dissolution. Based on the work of Swartz,[6] the stresses accompanying dissolution for the 30C° T-jump discussed above are estimated to produce a total of 0.12 cal of elastic strain energy per mole of Fe_3C dissolved. This should be compared to a calculated driving free energy change of −205 cal per mole of Fe_3C dissolved for the same 30C° T-jump. Thus, the driving force for dissolution is not appreciably altered by the strain energy generated during dissolution.

Thus far it has been assumed that the Fe_3C is stoichiometric and of constant carbon concentration, C_{CPD}. As a consequence, under the experimentally determined conditions of local nonequilibrium at the interface, the iron atoms would have to undergo a small but finite increase in chemical potential in moving from the Fe_3C to the ferrite (α). This would be avoided if the cementite were nonstoichiometric for a few atom layers in from the ferrite, the deviation being in the direction of decreasing carbon content and of such magnitude that the carbon in the Fe_3C is in equilibrium with the carbon in the ferrite at composition, C_s. This condition establishes local equilibrium with respect to carbon but not iron, and derives reasonability from the fact that the extreme mobility of interstitial carbon makes it doubtful that a discontinuity in μ_C exists at the interface. Since the free energy vs composition curve for Fe_3C is a "spike" (because of its near stoichiometry), the carbon concentration in the cementite will need to be only slightly lower than 6.67 wt pct in order to establish local carbon equilibrium, *i.e.* a small composition change causes a large change in $\mu_C^{Fe_3C}$. The magnitude of $\Delta\mu_C^{Fe_3C}$ necessary is simply $\Delta\mu_C^{\alpha} = \Delta\mu_C = RT \times \ln C_s/C_{eq}$, since $\mu_C^{Fe_3C}(6.67 \text{ wt pct}) = \mu_C^{\alpha}(C_{eq})$.

Using the Gibbs-Duhem equation in the Fe_3C, it is found that

$$d\mu_{Fe}^{Fe_3C} = -\left(\frac{N_C}{N_{Fe}}\right)_{Fe_3C} d\mu_C^{Fe_3C} \qquad [13]$$

where $(N_C/N_{Fe})_{Fe_3C}$ is the mole fraction ratio of carbon to iron in the Fe_3C. Since cementite is nearly stoichiometric and has the "spiked" free energy vs composition curve, $(N_C/N_{Fe})_{Fe_3C}$ is approximately

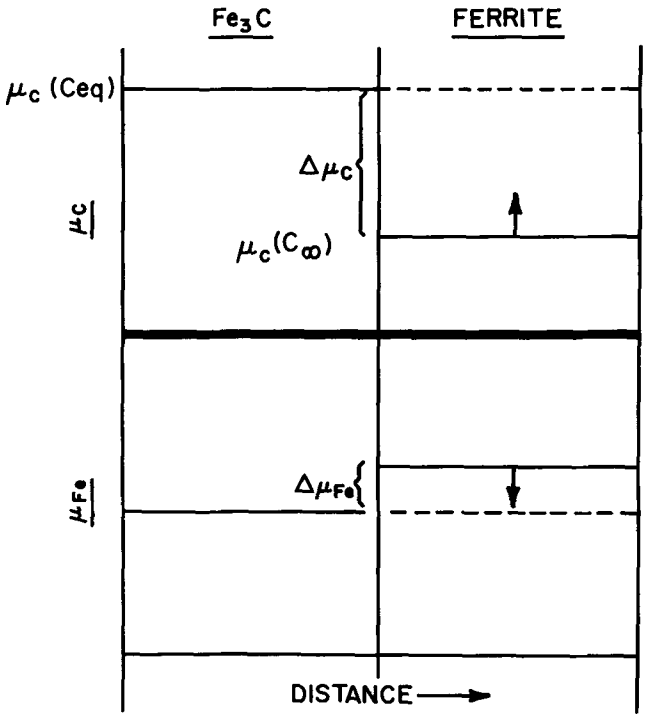

Fig. 4—Schematic diagram showing (*a*) $\Delta\mu C$ and $\Delta\mu Fe$ shortly after a 30C° T-jump for $K = 0$ and (*b*) the paths taken by μC and μFe during dissolution; stoichiometry is assumed in the Fe_3C.

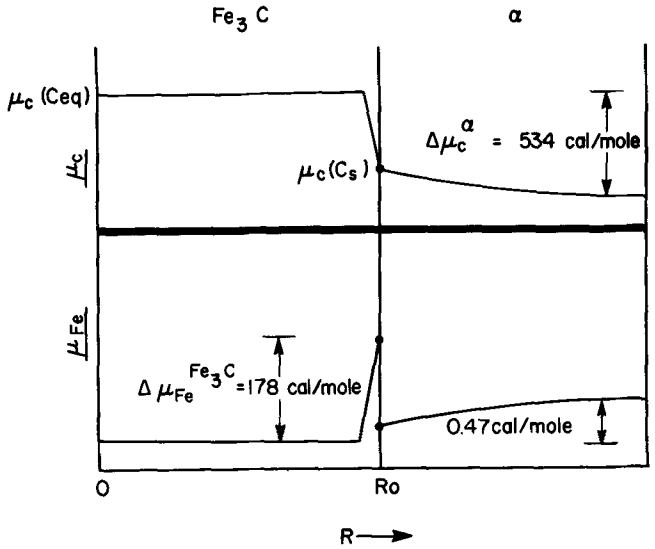

Fig. 5—Schematic diagram showing (*a*) $\Delta\mu C$ and $\Delta\mu Fe$ shortly after a 30C° T-jump for $K > 0$ and (*b*) the paths taken by μC and μ_{Fe} during dissolution; a nonstoichiometric surface layer is assumed in the Fe_3C.

constant and equal to 1/3 for not too large variations in $\mu_C^{Fe_3C}$. Thus Eq. [13] integrates to

$$\Delta\mu_{Fe}^{Fe_3C} = -\frac{1}{3}\Delta\mu_C^{Fe_3C} = -\frac{RT}{3}\ln\frac{C_s}{C_{eq}} \qquad [14]$$

Using Eqs. [9] and [14] and Fig. 4 it is found that the iron chemical potential-discontinuity, $\Delta\mu_{Fe}$, is now given by

$$\Delta\mu_{Fe} = RT(C_{eq} - C_s)\left[\frac{1}{21.4} - \frac{1}{3C_{eq}}\right] \qquad [15]$$

or since $C_{eq} \ll 21.4$

$$\Delta\mu_{Fe} \cong -\frac{RT}{3}\left[\frac{C_{eq} - C_s}{C_{eq}}\right] \qquad [16]$$

Using the previous example of a 30C° T-jump with $K = 0$, Eqs. [14] and [15] indicate that the establishment of local carbon equilibrium would result in $\Delta\mu_{Fe}^{Fe_3C}$ $= +534/3 = +178$ cal per mole, and $\Delta\mu_{Fe} \cong -(178 - 0.47)$ $= -178$ cal per mole. Fig. 5 shows schematically the chemical potential gradient at and near the interface shortly after a 30C° T-jump where it has been assumed that $K > 0$ and the diffusivities of carbon and iron in Fe_3C are very low.

The latter assumptions imply, under conditions of local carbon equilibrium and surface nonstoichiometry, that $\Delta\mu_C^{Fe_3C}$ (and hence $\Delta\mu_{Fe}^{Fe_3C}$) occurs over a short distance which gives rise to the steep chemical potential gradients shown; these gradients are sufficiently steep to appear as discontinuities.

As a result of the assumption of "surface nonstoichiometry," it is seen that iron moves down a chemical potential gradient and becomes the species involved in the interfacial reaction.

II) Mechanism

Consider an interphase boundary that is moving under some driving force subject to the assumption that the kinetics of motion are first order. The veloc-

ity, V, of the boundary is then given by

$$V = M\frac{\Delta\mu}{\delta} \qquad [17]$$

where M is the mobility of the boundary, and $\Delta\mu$ is the discontinuity in chemical potential of the reacting species across the boundary of thickness δ.

If it is assumed that a) $\Delta\mu_{Fe} \ll RT$, b) all surface atoms in the Fe_3C are available for jumping, c) iron atoms jumping from the Fe_3C to the ferrite do so independently of one another, and d) the jump process is a simple thermally activated one, then the local boundary mobility may be expressed by[7]

$$M = \frac{f\delta^2\nu}{RT}\exp\left(\frac{-\Delta G_m}{RT}\right) = \frac{D_m}{RT} \qquad [18]$$

where ν is a vibration frequency of the order of the Debye frequency, ΔG_m is the activation free energy for the jump process, $0 \leq f \leq 1$ is a factor introduced to account for the possibility that more than one jump per atom is necessary before a permanent site in the ferrite is found, and D_m is a "diffusion coefficient for boundary migration." Realizing that $\Delta G_m = \Delta H_m - T\Delta S_m$ where ΔH_m is the activation enthalpy and ΔS_m is the activation entropy, Eqs. [17] and [18] yield

$$V = \frac{\gamma f\delta\nu\Delta\mu_{Fe}}{RT}\exp\left(\frac{\Delta S_m}{R}\right)\exp\left(\frac{-\Delta H_m}{RT}\right) \qquad [19]$$

where γ is the areal fraction of sites in the ferrite to which iron atoms can jump.

Recalling that Fe_3C is a nearly stoichiometric compound, it is evident that

$$V = -\Omega J_{R=R_0} = \Omega K(C_S - C_{eq}) \qquad [20]$$

where Ω is the volume of cementite per mole of carbon, which when coupled with Eqs. [12], [16], and [19] yields

$$K = \frac{\gamma f\delta\nu}{3A\Omega}\exp\left(\frac{\Delta S_m}{R}\right)\exp\left(\frac{\Delta H_s - \Delta H_m}{RT}\right) \qquad [21]$$

where $\Delta H_s = 17.3 \times 10^3$ cal per mole is the heat of solution of cementite in ferrite, and A is a constant, (see Eq. [12], where $A = 1.29 \times 10^2$ in units of wt pct C).

Assuming that ΔH_m, ΔS_m, and ΔH_s are all independent of temperature, Eq. [21] is consistent with the observed variation of K with temperature shown in Fig. 2. It is clear that the observed Q's are, according to Eq. [21], given by

$$Q = -\Delta H_m + 17.3 \times 10^3 \qquad [22]$$

and that a positive Q is indicative of $|\Delta H_m| < 17.3 \times 10^3$ cal per mole.

Table II shows the values of ΔH_m calculated on the basis of Eq. [22]. The values of ΔH_m computed for the commercial purity specimens are not believed to be at all accurate since the value of ΔH_s used is for high purity Fe-C alloys and would most assuredly be affected by purity. For example, the manganese in the (C) alloys is known to decrease the activity of carbon[8] and hence the solubility of cementite. This can be associated with a larger value of ΔH_s.

Table II. Values of ΔH_m and Estimated Error Limits Computed from Eq. [22]

Sample	T_0, °C	ΔH_m, kcal/mole*
HP-QS	701	6.2 ±0 7
HP-QS	656	7.6 ±1.9
C-RS	701	0.3 ±2.9
C-RS	647	0.0 ±2.6
C-QS	698	–3.4 ±3.2

*The errors shown for ΔH_m are the probable errors given for Q. The actual uncertainty is greater by an amount equal to the error in ΔH_s, but since this was not given by Swartz[5] it is incalculable.

If the formalism expressed by Eq. [21] is to be at all realistic, it must be able to account for the displacement with T_0 of the data in Fig. 2. Such behavior can be explained by a temperature dependent preexponential term that has a large relaxation time when compared to the duration of an experiment, (1 sec).[2] The factor (γf) should be dependent upon the structural features of the interface, which may well be temperature dependent with a relaxation time considerably larger than 1 sec. The other preexponential terms are not sufficiently temperature dependent to account for the observed behavior.

The magnitude of (γf) can be estimated from Eq. [21] using the intercept data of Table I and the following parameter estimates:

$$\exp\left(\frac{\Delta S_m}{R}\right) \cong 1$$

$$\delta = 3 \times 10^{-8} \text{ cm}$$

$$\Omega = 24.3 \text{ cu cm per mole}^9$$

$$A = 0.84 \text{ moles per cu cm}$$

$$\nu = 10^{12} \text{ sec}^{-1}$$

Using a mean intercept value for specimen HP-QS ($\bar{I} = 7.9 \times 10^{-7}$ cm per sec), (γf) is estimated to be $(\gamma f) \cong 1.6 \times 10^{-9}$. Typically f is in the order of unity[7] so $\gamma \cong 1.6 \times 10^{-9}$. The precipitate radius in specimen HP-QS was 6.3×10^{-5} cm and corresponds to an area per particle of 5.0×10^{-8} sq cm which when multiplied by γ gives 8.0×10^{-17} sq cm as the area per particle of active jump sites. This should be compared to an estimated area per surface atom of 3.6×10^{-15} sq cm per atom.

The smallness of the area of active jump sites casts some doubt on the assumptions leading to Eq. [21], though lending support to the earlier hypothesis that interstitial carbon is in local equilibrium at the interface. This follows since γ for interstitial elements should be in the order of unity.

As an alternative to the above formalism for K, consider the following. Cementite is known to have an orthrombic crystal structure[4,10,11] with 4 formula weights per unit cell, while ferrite is bcc.* When occurring in the form of pearlite, Fe_3C and ferrite appear to have the orientation relationship[12]

$$(110)_\alpha \parallel \approx (001)_{Fe_3C}$$

$$[111]_\alpha \parallel [010]_{Fe_3C}$$

Carbides precipitated from martensite tempered at 400°C have been observed by Kelly and Nutting[13] to have the orientation relationship

*The lattice parameters (in Å) for Fe_3C and ferrite are.[10]

Fe_3C: $a_0 = 4.5235$, $b_0 = 5.0890$, $c_0 = 6\ 7433$

Ferrite: $a_0^{20\,°C} = 2.8662$, $a_0^{688°C} = 2.8944$

$(211)_\alpha \parallel (001)_{Fe_3C}$

$[0\bar{1}1]_\alpha \parallel [100]_{Fe_3C}$

$[1\bar{1}\bar{1}]_\alpha \parallel [010]_{Fe_3C}$

with the ferrite. For both of the above orientation relationships the degree of atomic matching between the two phases is quite good in the given directions. For example, there is only a 1.4 pct mismatch per unit cell along the b_0 axis of the Fe_3C and a $\langle 111 \rangle$ axis of the ferrite. It is conceivable, therefore, that there are a large number of regions of "coherent boundary" in the Fe_3C-ferrite interface and that the interface is, on an atomic scale, a network of interpenetrating ledges and kinks mingled among patches of coherent boundary which constitute the terrace areas. These areas are visualized as sharp interfaces having a large number of coincident sites and occasional misfit dislocations. The ledges and kinks are present to provide interfacial curvature needed for spherical particles and to accommodate regions of large atomic disregistry. Similar sorts of structures as these have been reported for grain boundaries in pure metals.[14]

The above suppositions concerning the interfacial structure describe boundaries that can conveniently be broken into the four basic types shown schematically in Fig. 6. Figs. 6(*a*) and 6(*b*) depict sharp coherent regions in both terrace and ledge configurations. Fig. 6(*c*) shows a situation where one phase is atomically flat and the other has ledges, and Fig. 6(*d*) shows a disordered region where ledges occur in both phases. The most likely areas for permanent atomic jumps to occur are those of the type shown in Fig. 6(*d*). Further, under low driving forces, kinks in the ledges will be the most favorable sites for atoms to both jump from and to. Let it be assumed, therefore, that a) atoms can make permanent jumps only in areas such as depicted in Fig. 6(*d*) (herein called "mobile regions"), b) the interfaces in these regions move normal to themselves *only* by the lateral motion of ledges, c) the ledges move normal to themselves *only* by the lateral motion of kinks, d) the atom jumps to and from kinks are thermally activated, and e) atoms will have permanent jumps in mobile regions *only* at sites having kinks in both phases as *near* neighbors. Fig. 7 shows a schematic representation of the assumed ledge-kink mechanism, where the boundary of the *i*th mobile region moves normal to itself with velocity, V_i, the ledges with velocity, $V_{i,l}$, and the kinks with velocity $V_{i,k}$. At "kink-pairs" the kink velocity, by analogy with Eq. [19] is given by

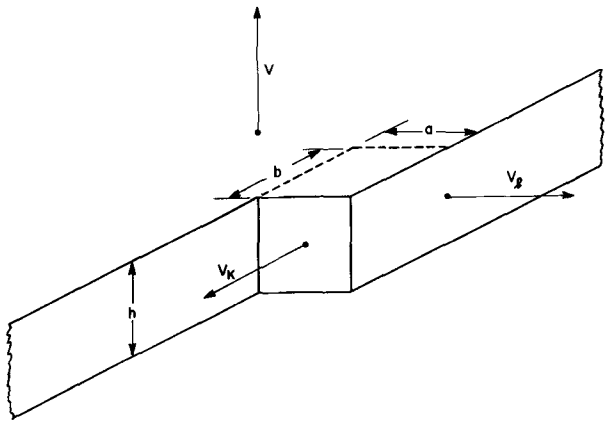

Fig. 6—Schematic diagram showing the four basic boundary types which can make up an interphase boundary. (*a*) Coherent boundary in terrace configuration. (*b*) Coherent boundary in ledge configuration. (*c*) Incoherent boundary with ledges in one phase and terraces in the other. (*d*) Disordered boundary with ledges in both phases.

Fig. 7—Schematic diagram of ledge-kink mechanism for interphase boundary migration.

$$V_{i,k} = f_i \nu_i b_i \exp\left(\frac{\Delta S_{i,m}}{R}\right) \exp\left(\frac{-\Delta H_{i,m}}{RT}\right) \frac{\Delta \mu_{i,Fe}}{RT} \quad [23]$$

From geometrical considerations, the ledge and surface velocities are given by

$$V_{i,l} = V_{i,k} a_i n_{i,kp} \quad [24]$$

where $n_{i,kp}$ is the number of kink-pairs per unit length of ledge in the *i*th mobile region, and

$$V_i = V_{i,l}\, l_i h_i \quad [25]$$

where l_i is the ledge length per unit area of the *i*th mobile region. Combining Eqs. [23], [24], and [25] under the assumption $a_i = b_i = h_i = \delta_i$, yields

$$V = \frac{1}{A'} \sum_i A_i' \frac{f_i \delta_i^3 l_i \nu_i \Delta \mu_{i,Fe} n_{i,kp}}{RT} \times \exp\left(\frac{\Delta S_{i,m}}{R}\right) \exp\left(\frac{-\Delta H_{i,m}}{RT}\right) \quad [26]^*$$

*A_i' as used in Eq. [26] and what follows is the area of the *i*th mobile region, and A' is the total surface area per particle.

Employing Eqs. [12] and [16] and using average quantities (denoted by lack of subscript) Eq. [26] becomes

$$V = \frac{(\gamma f)\, \delta^3 l \nu n_{kp} (C_s - C_{eq})}{3A} \times \exp\left(\frac{\Delta S_m}{R}\right) \exp\left(\frac{\Delta H_s - \Delta H_m}{RT}\right) \quad [27]$$

where γ is now the areal fraction of mobile regions. The average number of kink pairs per unit length of ledge in a mobile region is

$$n_{kp} = \frac{n_k^\alpha \cdot n_k^{Fe_3C}}{N} \quad [28]$$

where n_k^α and $n_k^{Fe_3C}$ are, respectively, the average number of kinks per unit length of ledge in ferrite and

cementite, and N is the average number of lattice sites per unit length of ledge; N is assumed to be approximately the same for both phases. Substituting Eq. [28] into Eq. [27] and using Eq. [20] yields for K,

$$K = \frac{(\gamma f)\,\delta^3 l \nu n_k^{\alpha} n_k^{Fe_3C}}{3A\Omega N} \exp\left(\frac{\Delta S_m}{R}\right) \exp\left(\frac{\Delta H_s - \Delta H_m}{RT}\right) \quad [29]$$

or, defining N_{kp} as the number of kink pairs per unit area of mobile region,

$$K = \frac{(\gamma f)\,\delta^3 \nu N_{kp}}{3A\Omega} \exp\left(\frac{\Delta S_m}{R}\right) \exp\left(\frac{\Delta H_s - \Delta H_m}{RT}\right) \quad [30]$$

For solid-gas interfaces that contain ledges n_k is a temperature dependent thermodynamic variable, the equilibrium number of which is given approximately by[15,16]

$$\frac{n_k}{N} \cong B \exp\left(\frac{-W}{RT}\right) \quad [31]$$

where B is a constant and W is the energy to form a kink and should be a fraction of the heat of vaporization.

Given that the relaxation time for equilibration of n_k in a solid-solid interface at temperature can be large compared to 1 sec, Eq. [30] is functionally consistent with the observed behavior of K with temperature in that N_{kp} decreases with decreasing temperature. In order to compare an estimated magnitude of the preexponential in Eq. [30] with the measured intercept data, let it be assumed that the mobile regions are sufficiently disordered and open that N_{kp} can be calculated by an equation of the form of Eq. [31]. It is clear, therefore that the magnitude of the discontinuous displacement of K with T_0, represented by $\Delta \ln(K)$, should be given by

$$\Delta \ln(K) = \Delta \ln(N_{kp}) = -\frac{(W^{\alpha} + W^{Fe_3C})(T_{0,1} - T_{0,2})}{R(T_{0,1})(T_{0,2})} \quad [32]$$

where terms other than N_{kp} are assumed approximately temperature independent. The mean value of $\Delta \ln(K)$ over the experimental temperature range for specimen HP-QS is $\overline{\Delta \ln(K)} = 0.18$.*

*$\overline{\Delta \ln(K)}$ is calculated by averaging the $[\Delta \ln(K)]$'s for a given specimen at the upper and lower temperature extremes of the data at $T_0 = 650°C$ and $T_0 = 700°C$. For example, the least squares slope and intercept of the data at $T_0 = 700°C$ is used to extrapolate the data into the range of the $T_0 = 650°C$ data, and vice versa.

Substitution of this into Eq. [32] along with $T_{0,1} = 650°C$ and $T_{0,2} = 700°C$ yields $(W^{\alpha} + W^{Fe_3C}) = W = 6500$ cal per mole. From Eqs. [29] to [31]

$$N_{kp} = lNB^{\alpha} B^{Fe_3C} \exp(-6500/RT) \quad [33]$$

which, assuming $B^{\alpha} \cong B^{Fe_3C} \cong 1$, $l \cong 10^5$ cm^{-1}, $N \cong 3 \times 10^7$ cm^{-1}, yields $N_{kp}^{700°C} \cong 9 \times 10^{10}$ cm^{-2}.

Using the $T_0 = 700°C$ intercept for specimen HP-QS and the various parameter estimates, $(\gamma f) \cong 1.5 \times 10^{-5}$. It is not difficult to imagine that more than one atom jump may be necessary before a kink pair can move. This would be especially true if the two kinks are separated by a few atom diameters. Given that one atom jump in ten is completed, then $f = 0.1$ and $\gamma \cong 1.5 \times 10^{-4}$ indicating that there is a relatively small areal fraction of particle surface where highly disordered interface exists. The area per particle of disordered interface is 7.5×10^{-12} sq cm which encompasses in the order of 2×10^3 atoms. This number is considerably more realistic than that which evolved from the earlier similar calculation.

A close connection between the mechanism of migration of interphase boundaries and grain boundaries would seem to be expected. However, there are significant differences between the present work and some reported grain boundary migration studies. Aust and Rutter[17,18] have investigated the effects of tin, orientation,[17] and temperature[18] on the rate of grain boundary migragion in lead. The driving force for migration was supplied by first growing a single crystal containing a lineage substructure, and then introducing a few (often one) recrystallized grains into the striated crystal. The driving force for growth of the recrystallized grain was constant and estimated at 2×10^{-2} cal per mole; this value should be compared to driving forces in the range of 30 to 180 cal per mole which were achieved in the present work.

They found that orientation had little effect on the migration rate if the tin concentration was less than 4×10^{-4} wt pct. However, for concentrations greater than this, (additions were made to 4×10^{-3} wt pct) the migration rate decreased rapidly with increasing tin content for randomly oriented grains and much more slowly for certain "special" orientations. These "special" orientations were such that the recrystallized grain and the striated crystal were related by a rotation of a) 36 to 42 deg about a common ⟨111⟩ direction, b) 23 deg about a common ⟨111⟩ direction, and c) 26 to 28 deg about a common ⟨100⟩direction. These "special" orientations have properties in common with the coherent type of interfaces discussed earlier in this paper.

The boundary velocity as a function of temperature at constant driving force was, for all orientations, adequately described by the relation

$$V = V_0(-Q'/RT) \quad [34]$$

where Q' was an apparent activation energy. However, it was found that the Q' values for random boundaries increased with increasing tin concentration and were always much larger than those of the "special" boundaries, which were observed to be independent of the tin concentration.* The Q' values for random orientations ranged from 15 to 43 kcal per mole and were constant at about 6 kcal per mole for the "special" orientations.

*These studies were made with tin additions to 2×10^{-3} wt pct.

Aust and Rutter calculated values of V at 300°C using Eq. [34] and the preexponential given by Eq. [19] ($\gamma f = 2 : Q' = \Delta H_m$) and found order of magnitude agreement between calculated and measured velocities for the "special" boundaries. However, calculated and measured velocities for the "random" and "intermediate" boundaries differed by 3 to 16 orders of magnitude, the calculated being too low. Since Eq. [19] does not include impurity effects, Aust and Rutter concluded that the formalism correctly described the elementary boundary migration process since it fit the data for the "special" boundaries which were insensitive to tin concentration. The disagreement between theory and experiment for the other boundaries was attrib-

uted to their sensitivity to impurities and the incapability of the theory to account for impurity-boundary interactions. This points out an essential difference between the results of Aust and Rutter's investigations and the present one, in that it has been demonstrated that the formalism leading to Eq. [19] does not fit the present experimental data. In addition, no evidence of a temperature dependent preexponential was found by Aust and Rutter though two anomalies were found in their plots of $\ln(V)$ vs $(1/T)$.[18] However, these could most easily be explained on the basis of slightly varying driving forces.

In contrast to the results of both Aust and Rutter and the present authors are those of Rath and Hu.[19] They found that high angle tilt boundaries (tilted about a common ⟨111⟩ axis) in wedge-shaped aluminum bicrystals migrated with a velocity which could be described as a power function of the driving force; the exponent decreased from 4 for a 40 deg boundary to 3.2 for a 16 deg boundary. It is clear from these results that a first order process or processes do not dominate the migration of the bicrystal boundary. The driving forces ranged from 2.4×10^{-4} to 1.2×10^{-3} cal per mole and it was found that the boundary velocity was nearly independent of orientation for the lower driving forces and increased with increasing misorientation for the higher driving forces. In addition, it was found that the activation energy decreased with increasing driving force and varied only slightly with orientation.

The ledge-double kink mechanism proposed in this paper explicitly requires that iron atoms jump from the Fe_3C to the ferrite *only* at sites having kinks in *both* phases as *near* neighbors. This requirement precludes the possibility of any diffusion of iron along the Fe_3C-ferrite interface. Stated another way, the mechanism requires that interphase boundary diffusion of iron be difficult. It is precisely this feature of the proposed mechanism which enables it to account for the low preexponential values obtained experimentally, and it is also this feature which differs most significantly from the usual grain boundary migration theories.[7,20,21] A theory recently advanced by Gleiter[21] explicitly assumes boundary diffusion to take place and would not, therefore, be able to account for the present experimental findings.

SUMMARY

The following conclusions have been made:

1) The dissolution of Fe_3C in ferrite is controlled by a slow first order interfacial reaction.

2) The reaction rate constant, K, is Arrhenius in behavior and involves two activation enthalpies; one applies to a jump process with a short relaxation time, another to a long relaxation time process which is tentatively identified as a change in kink density on ledges in the interface. The heat of solution of Fe_3C in ferrite also appears in the exponential.

3) A single process, activated jump theory is not adequate to explain the behavior of K with temperature.

4) A dissolution model based on a ledge-double kink mechanism appears to be in agreement with experiment.

5) The Fe_3C-ferrite interface is felt to be at equilibrium with respect to carbon but not iron, leading to small departures from stoichiometry in the Fe_3C at the interface.

ACKNOWLEDGMENTS

The authors wish to thank Drs. R. H. Spitzer, Jr. and K. Natesan for many helpful and stimulating discussions of this work, the Office of Naval Research and the National Steel Corp. for partial financial support, and the U. S. Steel Corp. for material. The comments of Drs. M. F. Ashby and Kurt Lücke are also gratefully acknowledged. A portion of this work was performed under the auspices of the United States Atomic Energy Commission.

REFERENCES

1. F V. Nolfi, Jr., P. G. Shewmon, and J. S Foster: *Trans. TMS-AIME,* 1969, vol. 245, pp. 1727-33.
2. F V. Nolfi, Jr., P. G Shewmon, and J. S Foster: *Met. Trans.,* 1970, vol. 1, pp. 789-800.
3. H. Margenau and G. M. Murphy. *The Mathematics of Physics and Chemistry,* D. Van Nostrand Company, Inc , 1956.
4. L. S Darken and R. W. Gurry: *Physical Chemistry of Metals,* McGraw Hill Book Co., New York, 1953.
5. J. C. Swartz: *Trans. TMS-AIME,* 1969, vol. 245, pp. 1083-92.
6. J. C. Swartz: *Trans. TMS-AIME,* 1967, vol. 239, pp. 68-75.
7. K. Lücke and H. P. Stüwe: *Recovery and Recrystallization of Metals,* pp 171-210, Interscience Publishers, 1963
8. R. P. Smith: *J. Am. Chem. Soc.,* 1948, vol. 70, pp. 2724-29.
9. R. W Heckel and R. L DeGregorio *Trans. TMS-AIME,* 1965, vol 233, pp. 2001-11.
10. W B. Pearson: *Handbook of Lattice Spacings and Structures of Metals–Vol. 2,* pp. 427-28, Pergamon Press, 1967.
11. L. J. E. Hofer. U.S. Bur. Mines Bull. 631, 1966.
12. L. S. Darken and R. M. Fisher. *Decomposition of Austenite by Diffusional Processes,* pp. 249-94, Interscience Publishers, 1962.
13. P. M. Kelly and J Nutting: *J. Iron Steel Inst.,* 1961, vol. 197, pp. 199-211.
14 H. Gleiter: *Acta Met.,* 1969, vol. 17, pp. 565-73.
15. J. P. Hirth. *Energetics in Metallurgical Phenomena–Volume II,* pp. 1-52, Gordon and Breach Science Publishers, 1965.
16. W. K. Burton, N Cabrera, and F. C Frank: *Phil Trans. Roy. Soc.,* 1951, vol. 243A, pp. 299-358
17. K. J. Aust and J. W. Rutter: *Trans. TMS-AIME,* 1959, vol. 215, pp. 119-27.
18. K. J. Aust and J W. Rutter: *Trans. TMS-AIME,* 1959, vol. 215, pp. 820-31.
19. B B. Rath and Hsun Hu· *Trans. TMS-AIME,* 1969, vol. 245, pp. 1577-85.
20 D. Turnbull: *AIME Trans.,* 1951, vol. 191, pp 661-65.
21. H. Gleiter: *Acta Met.,* 1969, vol. 17, pp. 853-62.